Magnetotelluric and Seismic Joint Inversion using Nelder-Mead Minimization

Thesis submitted in accordance with the requirements of the University of Adelaide for an Honours Degree in Geophysics.

Simon Carter

November 2012

THE UNIVERSITY
of ADELAIDE

ABSTRACT

It is often assumed that the combination of geophysical data within a single inversion framework yields a geologically more robust and reliable model than can be obtained from separate individual inversions. In this study this assumption is questioned with specific reference to magnetotelluric (MT) and seismic data. Forward modelling, incorporating the Nelder-Mead parameter optimization method, is used to test the hypothesis that zones with similar reflectivity represent geological zones with similar electrical properties. This is a new, geometric approach, to joint inversion. Subsurface structures at a potential mine site are examined using seismic and MT inversion results, and aspects of the deposit are interpreted from the perspective that preconceptions and assumption influence the results of joint inversion. A number of statistical techniques are then employed to examine if the geological processes that produce changes in elasticity also have some impact on resistivity. The two dimensional seismic reflection and MT data used to examine these concepts are from the Hillside Project Area, Yorke Peninsula South Australia.

KEYWORDS

joint, inversion, magnetotelluric, seismic, Nelder, Mead, simplex, Hillside

Table of Contents

List of Figures

INTRODUCTION

The literature on joint inversion falls into three broad categories: inversion of identical or near identical physical properties (Vozoff & Jupp 1975a; Vozoff & Jupp 1975b; Raiche et al. 1985); joint inversion when there is a statistical, theoretical or empirical relationship between dissimilar types of data (Pilkington 2006; Constable et al. 1987; Bosch 1999; Hoversten et al. 2006; Michael Hoversten et al. 2007); and, joint inversion when there is a structural link between the data (Haber & Oldenburg 1997; Gallardo & Meju 1997a; Gallardo & Meju 2004; Gallardo & Meju 1997b; Gallardo et al. 1997; Linde et al. 2006; Tryggvason & Linde 2006; Linde et al. 2008; Hu et al. 2009; Gallardo 2007; Fregoso & Gallardo 2009; Gallardo & Meju 1997a; Gallardo & Meju 2004; Gallardo & Meju 1997b; Gallardo et al. 1997; Linde et al. 2006; Tryggvason & Linde 2006; Linde et al. 2008). However, a definitive method that produces conclusively better results in all but specific and limited cases does not yet exist. Indeed, very little has been written regarding the shortcomings of joint inversion, even though it is commonly assumed the method leads to improvement of interpretation.

There are a number of factors that influence the results of joint inversion, depending on the particular combination of data selected and on the methods used. These include:

- data weights are usually required, but no clear selection rules exist;

- for iterative methods the starting points may influence the final model outcome;

- non-linearity and the risk that the solution might iterate towards the wrong local minima; and,

- how should roughness be defined for data with different intrinsic sensitivities?

The aim of this study is to begin to assess these factors and to question the assumption that joint inversion leads to better results. Subsurface structures at a potential mine site

will be examined using seismic and MT inversion results, and aspects of the deposit will then be interpreted from the perspective that preconceptions and assumption influence the results of joint inversion. This study will examine the co-dependence of different types of geophysical information that are often combined in joint inversion processes, but with a specific focus on seismic and MT data. The 2D seismic reflection and 2D MT data used to examine these concepts are from the Hillside Project Area, Yorke Peninsula South Australia.

REVIEW

Joint inversion is the process of taking two or more types of geophysical information, such as density, magnetic susceptibility, elastic and electrical properties, and combining them in such a way that a physical characteristic of the Earth is determined with more accuracy than could be obtained by analysing each data set individually. It is a challenging problem because inversion problems are frequently ill-posed; that is the problems are non-linear and have non-unique and unstable solutions. Ill-posed can also mean that there are more parameters than there are data points to constrain them. In addition to the issues of being ill-posed, joint inversion problems have an extra element of complexity. For the methods to be effective, there needs to be an inter-dependence, so that one method can provide additional information in quantifying the second. However, because joint inversion can help pick-out the best solution of many, the inherent challenges are worth resolving. The number and breadth of publications cited in recent reviews (Haber & Holtzman Gazit 2012; Gallardo & Meju 2011) show that the integration of different types of geophysical and geological data through joint inversion is an important and continuously evolving discipline.

We can simplify geophysical processes by making the following statements. There are six primary physical properties of geophysics: magnetic susceptibility κ, density ρ, complex resistivity ρ' (which is a combination of electrical resistivity and dielectric permittivity), and the three elastic parameters K, μ, ν for bulk modulus, shear modulus and Poisson's constant respectively. Furthermore, geophysical modelling can be summarized through three types of partial differential equation (PDE): elliptical, parabolic and hyperbolic. Elliptical equations involve only spacial variables and are used to model gravitational and magnetic potentials. Parabolic equations include a first order time dependent term and are used to model diffusive processes such as the dispersion of heat and the evolution of electromagnetic fields. Hyperbolic equations include a second order time dependent term and are used to model wave propagation. Combining these broad statements: there are six primary properties of interest that are incorporated into three types of PDE to model the basic processes of geophysics.

The six parameters of geophysics are linked in a number of ways. There may be a direct equational link, such as Poisson's relationship between gravity and magnetism (Telford et al. 1990). In other cases there is a petrophysical link, such as the way both density or electrical resistivity are a reflection of porosity (Maier 2011). There also may be a structural link, such as the way changes in elastic modulii between Earth boundaries may relate to similar changes in other geophysical properties. This last link is particularly relevant to this investigation, where the focus is on seismic and MT data.

These links are exploited in joint inversion to obtain more plausible geological models. Generally, it is easier to conduct joint inversion with techniques that are sensitive to the same physical properties, such as MT and DC resistivity data (Vozoff & Jupp 1975a), or when there is a direct equational link (Pilkington 2006). MT and seismic information

are particularly difficult to combine since electrical resistivity and elastic moduli are not intrinsically related. Often, seismological data are not inverted, and the interpretation is undertaken subjectively based upon two-way travel time data. This problem is compounded in the case of hard rock seismology, where regions of different rock type are only weakly differentiated in many cases.

Some of the issues that arise when attempting to incorporate information into the inversion process, especially structural information, can be explained by taking a more formal approach. Consider two sets of geophysical data d and d', two kernel functions F and G that link model parameters to data with some uncertainty ϵ, and the associated forward problems:

$$F(m) + \epsilon = d \tag{1}$$

$$G(m') + \epsilon = d' \tag{2}$$

Solving the inversion problem involves inverting Equation 1 (or Equation 2) to find the model function m (or m'). A distinction is made by Haber & Holtzman Gazit (2012) between *model fusion* and joint inversion. If it is first assumed that m' has similar structure to m, then it is possible to define the incorporation of information about m' into m as model fusion. In contradistinction, joint inversion is specifically defined as incorporating information about m' into the inversion of m and vice versa. Given these definitions, problems arising from inverting several types of information are summarized by Haber & Holtzman Gazit (2012) as:

- m and m' measure different quantities and have different units (or in the case of a geological model, m and m' may be unit-less);

- there may be no known correspondence map between m and m'; or,

- m and m' have similar structure in some regions but not others.

It is also known that the best mathematical solution may be one that is geologically impractical (Parker & Whaler 1981). For example, an infinitesimally thin conduction layer that stretches to infinity in the plane may be the best mathematical solution to one dimensional MT inversion, despite being physically unrealistic. This issue, and some of those previously outlined, can be examined using forward modelling, with the objective of highlighting the problem of convergence to the wrong solution.

Since joint inversion depends upon a connection between the data, it is reasonable to consider what happens when joint inversion does not improve the model. This leads us also to ponder in what sense the new model is not better and to question if the assumptions made for joint inversion are always appropriate. If the results from conducting joint inversion are poor, this may provide evidence that the assumed physical interdependence does not exist.

APPROACH

Forward modelling is our key tool in analysing the benefits and pitfalls of joint inversion. Closed-form solutions exist for the surface gravity response of simple geometric bodies such as spheres, cylinders, slabs and dykes (Telford et al. 1990) that can be used to establish forward models. The magnetic response at the surface can be modelled using the density profiles and Poisson's relation between gravity and magnetic potential (Telford et al. 1990). Such models can then be used to test assumptions about joint inversion. Simple, closed form solutions to forward model the surface MT response to subsurface resistivity structures exist for one-dimensional and a few, limited two-dimensional cases,

but completely general equations do not exist. We therefore need to rely upon mathematical approximation. The techniques used in our investigation to calculate the surface MT response make use of finite element methods.

Ideally we want to know if joint inversion will give better results, and the considerable literature on joint inversion encourages the belief that improvements over single inversion are possible. We will consider MT and seismic results. The testable question is: do zones of similar reflectivity represent geological zones of similar electrical properties? In other words, do the geological processes that produce changes in elasticity also have some impact on resistivity? The exact cause of such a connection is not our concern here. If there is a boundary between two lithofacies, and on each side of the boundary there are different seismic velocities and different electrical resistivities then, regardless of the reason, we can answer in the affirmative.

The Downhill Simplex Method

The Nelder-Mead Method (Nelder & Mead 1964), often referred to as the *Downhill Simplex Method*, is an optimization technique for a function of several variables that does not make use of derivatives, since it only requires evaluation of the function. A simplex is a convex hull with n+1 vertices in n-dimensional space. It is a generalization of the triangle to higher dimension, so that in two-dimensional space the simplex is simply a triangle and in the three-dimensional space it is a tetrahedron. If we consider the case of two variables, the Nelder-Mead Method involves calculating the value of the function we wish to minimize at the three vertices. A vertex is defined by parameter values $\{M_i, i = 1, ..N\}$, where each vertex has a slight perturbation in one parameter. For the two variable case, the vertices could be written $\{(M_1, M_2), (M_1 + \Delta, M_2), (M_1, M_2 + \Delta)\}$.
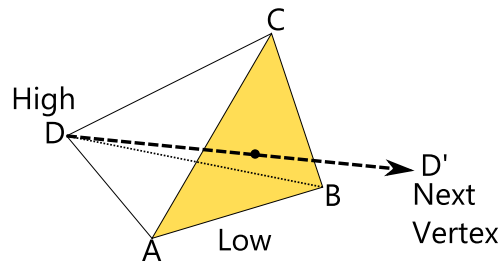
Figure 1: Simplex tetrahedron for the three-dimensional case, showing the position of the next vertex since the value of the function at D is greater than the value of the function at the other vertices A, B and C. Complimentary rules exist for expanding the tetrahedron in a single, consecutively minimizing direction, or for contracting down upon the optimal solution.

The vertex where the calculated value of the function is greatest is removed, and a new vertex is chosen by reflecting the triangle along the edge of the other two vertices in the case of two-variables (or through the hyper-plane created by the other vertices in higher dimensional problems). The search continues by evaluating the function at the new vertex, comparing it to the leftover vertices from the previous iteration and moving in a new direction. Complimentary rules exist for expanding the triangle in a single, consecutively minimizing direction, or for contracting down upon the optimal solution. Figure 1 shows a simplex in three dimensions, with D, the vertex with the highest calculated value, replaced by D'. If our model had only three zones of resistivity, then this simple tetrahedron would crawl around in the model space, moving towards the minimum. At each vertex, the value of the function we calculate, and try to minimize, is the RMS error between the model and the soundings (MT responses). A more general exposition of the method is given in (Press et al. 2007).

The Algorithm

We would like to establish areas of coincident seismic and electrical resistive behaviour, or provide evidence to confirm where such a link is weak. An approach to calculate sur-

face MT resistivity and phase values at each frequency, that would result from a specified subsurface resistivity profile, is found in (Wannamaker et al. 1987). These forward model values can be compared to the MT responses, called *soundings data* in WinGLink (we shall use the terms MT responses and soundings data interchangeably). WinGLink is software that performs non-linear conjugate gradient inversion by employing the algorithm described in (Rodi & Mackie 2001). These soundings are the resisitivity and phase values at each site and each frequency that results from transforming the $\mathbf{E}$ and $\mathbf{B}$ field measurements taken during the MT survey. This transformation can be done by first using **BIRRP** (Bounded Influence Remote Reference Processing) (Chave & Thomas 2003) to create impedance tensors from the field measurements, and then using a subroutine within WinGLink to evaluate resistivity and phase values. Although a transformation from the initial $\mathbf{E}$ and $\mathbf{B}$ measurements is involved, we can think of resistivity and phase values for each frequency (the soundings data of WinGLink), as the measured surface MT response. By systematically changing the initial resistivity values in each region (imposed over the inverted seismic and MT profiles as a grid of alphanumeric zones, see Figure 7), it is possible to establish the best matches between the:

- MT responses (soundings data) and the seismic model.

- MT responses and the block MT model.

The best match is achieved by minimizing χ^2 for errors between the MT responses and the forward modelled surface MT resistivity and phase values, calculated on the basis of the imposed seismic and MT regions. A method to achieve this minimization was proposed in (White & Heinson 1994). This paper makes use of the Nelder-Mead Method to achieve the minimization. A schematic outline of the approach is given in Figure 2.
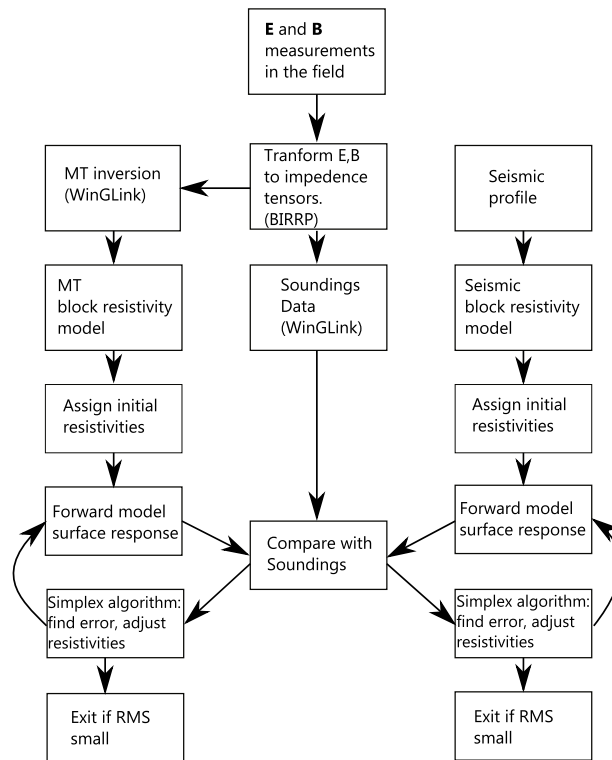
```
                              ┌──────────────┐
                              │ E and B      │
                              │ measurements │
                              │ in the field │
                              └──────────────┘
                                     │
                                     ▼
┌──────────────┐            ┌──────────────┐        ┌──────────────┐
│ MT inversion │ ◄───────── │ Tranform E,B │        │ Seismic      │
│ (WinGLink)   │            │ to impedence │        │ profile      │
│              │            │ tensors.     │        │              │
└──────────────┘            │ (BIRRP)      │        └──────────────┘
       │                    └──────────────┘               │
       ▼                           │                        ▼
┌──────────────┐            ┌──────────────┐        ┌──────────────┐
│ MT           │            │ Soundings    │        │ Seismic      │
│ block        │            │ Data         │        │ block        │
│ resistivity  │            │ (WinGLink)   │        │ resistivity  │
│ model        │            │              │        │ model        │
└──────────────┘            └──────────────┘        └──────────────┘
       │                           │                        │
       ▼                           │                        ▼
┌──────────────┐                   │                ┌──────────────┐
│ Assign initial│                  │                │ Assign initial│
│ resistivities │                  │                │ resistivities │
└──────────────┘                   │                └──────────────┘
       │                           │                        │
       ▼                           ▼                        ▼
┌──────────────┐            ┌──────────────┐        ┌──────────────┐
│ Forward model│ ───────►   │ Compare with │  ◄──── │ Forward model│
│ surface      │            │ Soundings    │        │ surface      │
│ response     │            │              │        │ response     │
└──────────────┘            └──────────────┘        └──────────────┘
       ▲ │                                                ▲ │
       │ ▼                                                │ ▼
┌──────────────┐                                  ┌──────────────┐
│ Simplex algorithm:│                              │ Simplex algorithm:│
│ find error, adjust│                              │ find error, adjust│
│ resistivities     │                              │ resistivities     │
└──────────────┘                                  └──────────────┘
       │                                                  │
       ▼                                                  ▼
┌──────────────┐                                  ┌──────────────┐
│ Exit if RMS  │                                  │ Exit if RMS  │
│ small        │                                  │ small        │
└──────────────┘                                  └──────────────┘
```

Figure 2: Flow chart showing the approach. To examine the testable question we create two block models of subsurface resistivity, one based on the inverted MT profile and the other based on the seismic profile. The two profiles are compared by first assigning a symbol (either a number or letter) to each zone of the block models, and each symbol is then assigned an initial resistivity, which is used for forward modelling the surface MT measurements. The Nelder-Mead method is used to find the best combination of subsurface resistivities that most closely match the forward model and the MT response (which are the soundings data calculated through WinGLink).

Analysis

The method outlined above will result in two resistivity profiles (one for the seismic section and another for the MT block model), an RMS error between each of these models and the soundings data, and a set of resistivity and phase values for the TE and TM modes. TE refers to *transverse electric* so that current measurement is oriented along strike, while TM is *transverse magnetic*, with magnetic measurement oriented along strike. Depending upon the orientation of resistivity boundaries, one mode will likely provide superior results. The three sets of resistivity and phase values can then be plot-

ted against period for the purpose of comparison and in order to examine the question: do the geological processes that produce changes in elasticity also have some impact on resistivity?

While the three sets of resistivity and phase values, plotted against period, provide a good comparison at each instrument location, a better global picture is attained by examining residuals data. We can plot the residuals with a coloured scale versus period, along the length of the seismic line, for both resistivity and phase. A good model is indicated by a uniform colour band for low residual errors. With this visual presentation we can instantly recognize specific sites or frequencies where there is a significant model mismatch. We would also like to know something about the sensitivity of the solutions to perturbations, since it will give an indication of the stability of a solution and can also show if a better solution exists. This can be achieved by running the simplex algorithm for a single iteration, using the optimal solution for the initial zone values. By systematically changing one pair of values, we can create a contour plot of RMS errors for those two zones, all other zones kept equal. An example of this is given in Figure 10.

CASE STUDY

The study involved interpreting some aspects of a copper-gold ore deposit below shallow cover rocks at Hillside, Yorke Peninsula South Australia. Over eight days in March and a further three days in July 2012, MT data were collected at 65 sites. This covered an area approximately 2 km by 1 km overlaying the dominant magnetic anomaly, with an inter-site spacing of 250 m. A higher resolution MT survey along the single 2D seismic line available, with instrument spacing of 50m, was also conducted. Other geophysical survey results including seismic, gravity and magnetic potential figures were made avail-
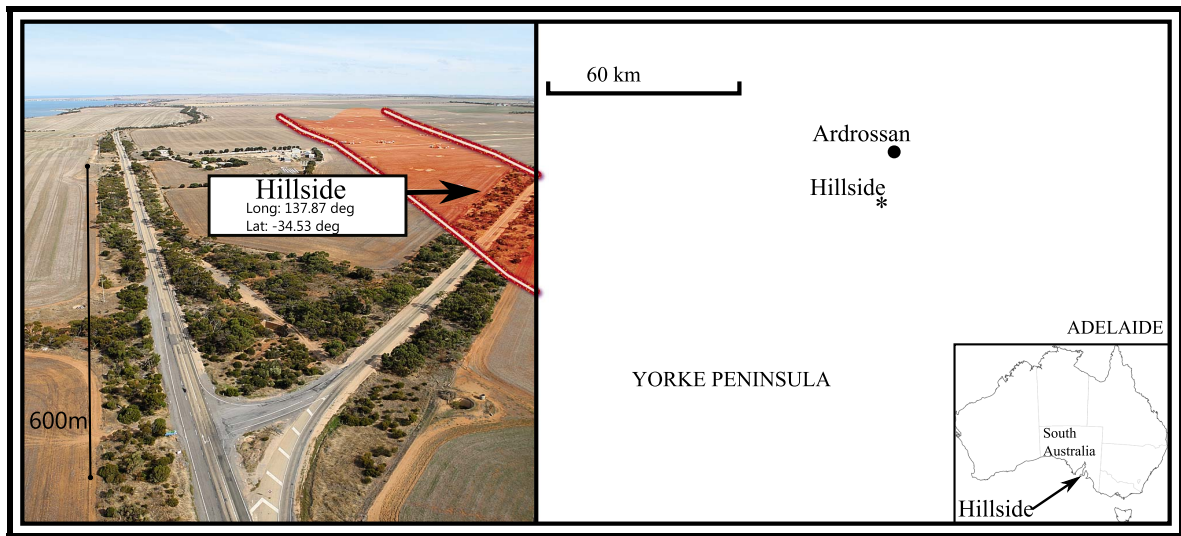
Figure 3: Location of the Hillside Project Area, Yorke Peninsula South Australia.

able, courtesy of Rex Minerals, the owners of the mining lease.

The seismic profile in Figure 4 was provided by staff at Curtin University. A number of regions of interest have been marked using blue and black outline. The similar rock velocities between the different lithofacies means reflective boundaries are not always obvious, and the division is predominately based upon the identification of areas with consistent reflective characteristic (patterns of similar amplitude or signal attenuation).

Pseudo-sections for apparent resistivity and phase, for both TE and TM modes, are shown in Figure 5. The data show variation in both modes along the line, particularly the TM mode, consistent with a complex subsurface. As Hillside is an industrial site, the time series data had a strong 50 Hz (and harmonics) signal present, which was removed with a notch filter. However, there is still noise in the data, which will impact on the final RMS error of any fitted model. Due to problems with the signal, sites 10 and 12 were omitted in undertaking the inversion to produce the two-dimensional MT profile
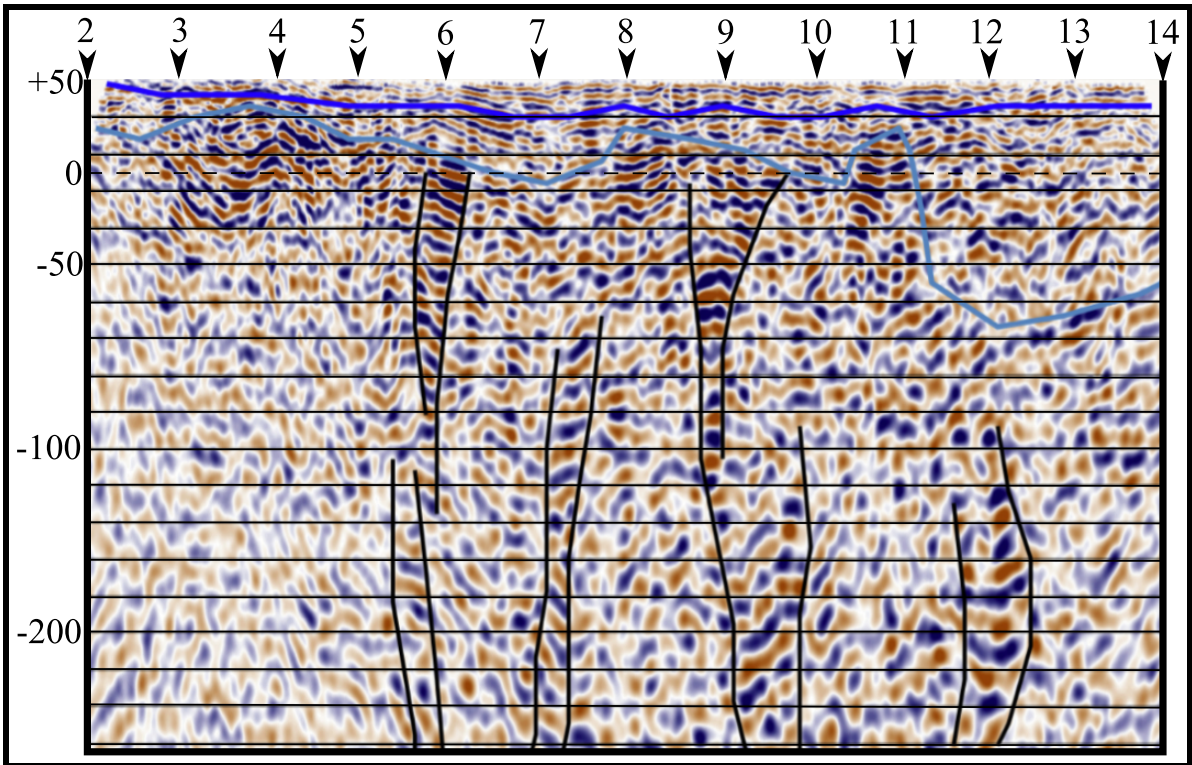
Figure 4: The seismic line, with region having similar seismic characteristics outlined. The boundaries are used to create a forward model for MT response based on zones of similar elastic behaviour. The similar rock velocities between the different lithofacies means reflective boundaries are not always obvious. The division is likely based upon the identification of areas with consistent reflective characteristic (patterns of similar amplitude or signal attenuation), with drilling results providing guidance.

of Figure 6.

Prior knowledge of the geometry of the deposit orientation at Hillside was used in planning the location and orientation of the MT instruments. For the Hillside survey, the TM mode has the magnetic measurements oriented geographic North (strike) and the electric field measurements oriented geographic East, while the TE modes has magnetics across strike and electric field along strike. Dimensionality analysis confirmed there is dominant strike, and data are predominately 2D, based on $skew < 4 \deg$, for periods less than 50 seconds.
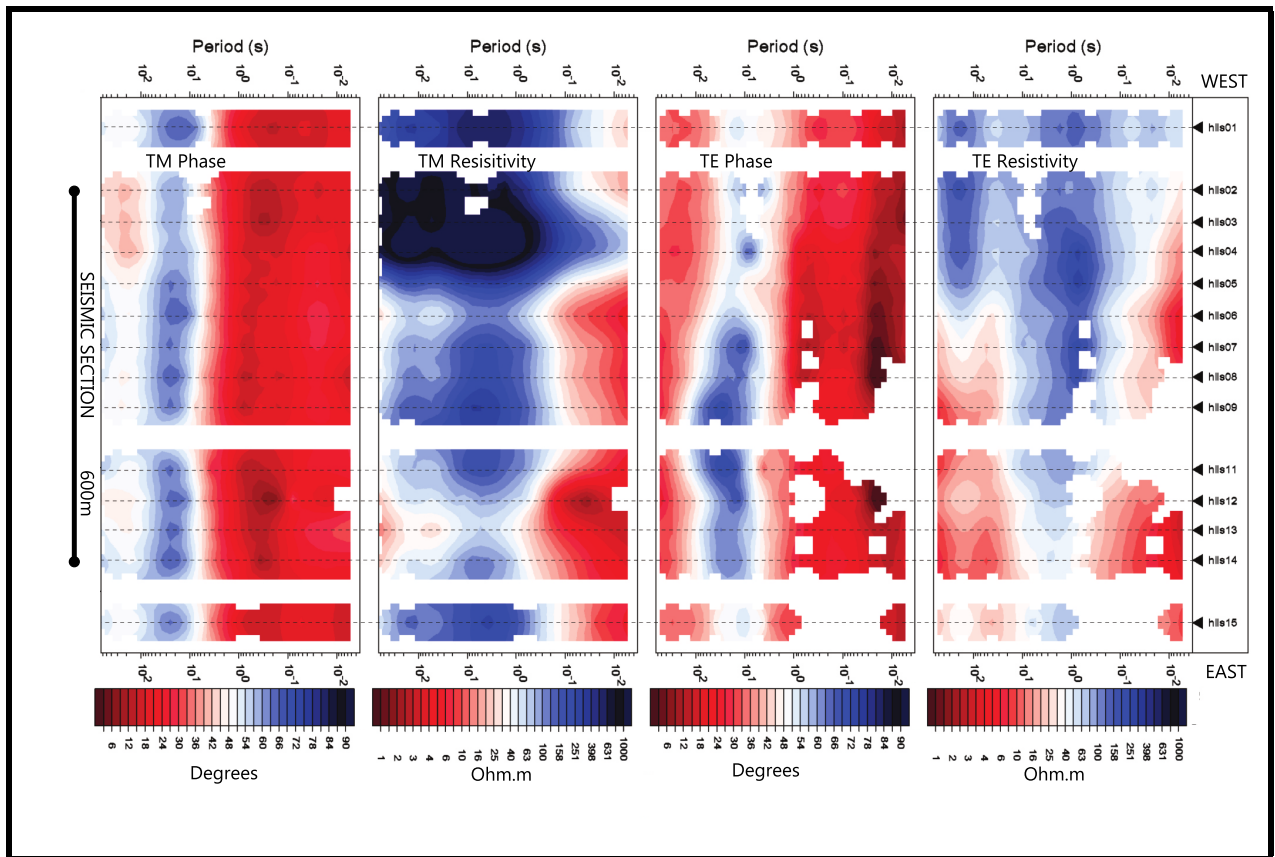
Figure 5: Pseudo-sections for resistivity and phase for both TE and TM modes for all sites. Hillside is an industrial site, and noise from drilling rigs, machinery and electrical power cables impacted on the quality of the data.

After processing the MT data coincident with the seismic line, WinGLink was used to undertake the inversion that produced the two-dimensional resistivity profile. The parameters chosen were $\tau = 1$ (decreasing from $\tau = 50, 20, 15, 10, 5$ to produce a smoother model), $\alpha = 1$, $\beta = 2$, $\tau = 1$, with iteration proceeding until RMS=1.5. The inversion is for short periods only, that is periods less than 1 second. The resulting 2D MT profile at Figure 6 identifies regions with similar resistive characteristics.

A number of regions are highlighted on Figure 6. These are chosen on the basis of marking out distinct MT responses. The first observation is that there is approximately a 1:1000 difference in the range of resistivity values. Secondly, while some regions, such
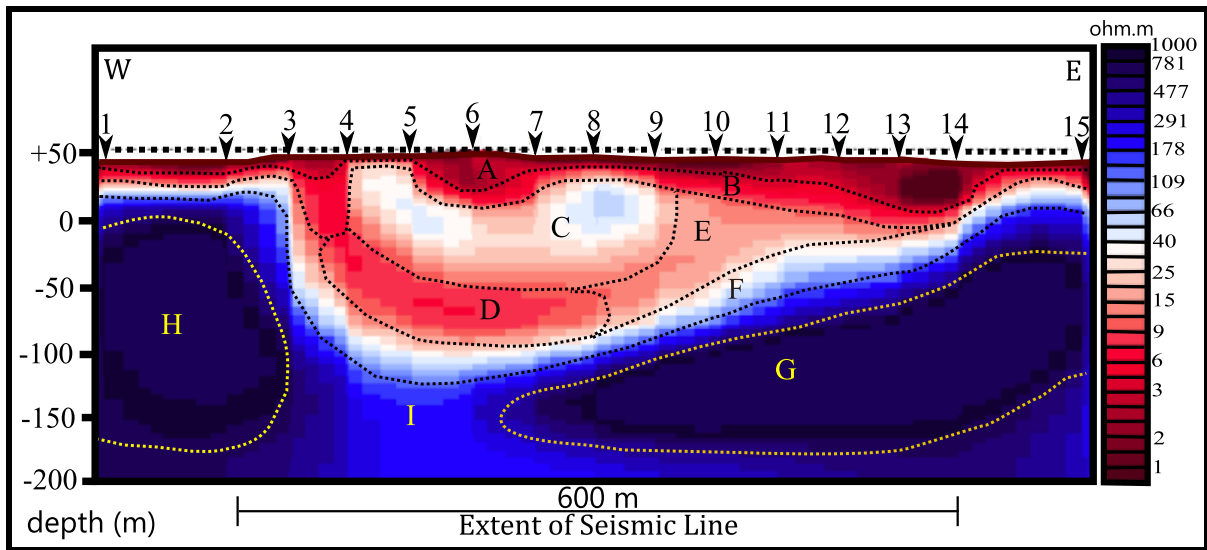
Figure 6: Inverted MT resistivity profile. There are 15 sites in total, with 50 metre intervals between sites 2-14 and 100 spacing to the end sites at 1 and 15. Sites 10 and 12 were not used in the inversion, due to excessive noise in the data. The seismic measurements begin at MT site 2 and end at 14, so that the first and last set of MT instruments are outside the area covered by the seismic survey. The zones were assigned on the basis of similar resistivity values. While for some zones such as those marked G and H, the boundaries appear quite distinct, the division between other zones is less clear.

as those marked G and H appear quite distinct, the boundary between regions A and B is more arbitrary. Thirdly, the boundary at C and E appears quite distinct according to the resistivity colour profile, but region E resistivity may be as little as 30% less than C, which is almost insignificant when compared to the one-thousand fold difference between regions A and H. Preconception about what is and what is not a boundary will have some impact on the inversion results. A visual comparison of the MT and seismic profiles also indicates a strong match both at what would appear to be the regolith lower boundary and then at the weathered layer (often taken as the layer above the water table). These zones are highly conductive, due to the high water content. While the seismic boundaries are not always clear across the entire length of the survey, the delineations in resistivities at the upper layers appear well defined.

Figure 7: Example of a small section of the geometric input into the simplex algorithm taken from the MT model. This shows the division of a section of the MT profile into several zones. The same process is applied to the seismic profile to create the MT forward model based upon zones of similar elastic behavior.
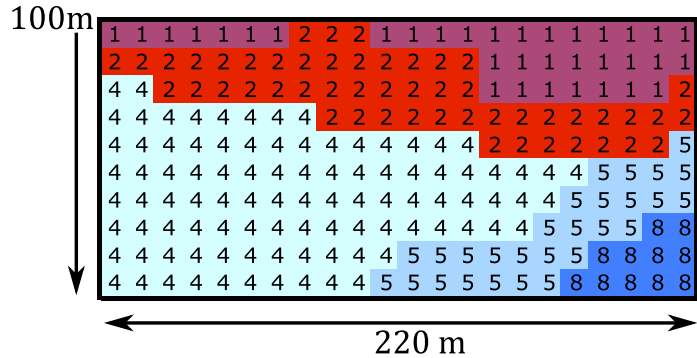
Figure 4 and Figure 6 were used to create a resistivity model below the seismic line, down to a depth of 500 metres. This was achieved by imposing a grid with 138 columns and 76 rows over the the MT and seismic profiles and then assigning a letter or number to each node based upon zones of similar resistive or elastic behavior. A division of up to 35 geophysical regions is permitted by the software, comprising the first 9 numbers along with the 26 letters of the alphabet. This mesh of resisitivity values is the geometric input into the algorithm used to forward model the surface MT response and minimize χ^2. An example section is given in Figure 7.

Following the steps outlined in the *Approach* section leads to the creation of Figure 8, which are plots of the MT response (soundings) versus the MT block model and the MT response versus the seismic block model. These plots are spread across the full width of the seismic line, providing a comprehensive sample of the results. The RMS error for the MT model was 4.91 and 7.62 for the seismic model. It is evident that the MT model closely matches the soundings resistivity and phase values. In comparison, the seismic model gives a poor match.

DISCUSSION

Comparison of Models

Figure 8 shows the MT responses (soundings data) and simplex outputs from the MT and seismic models. The TM mode provides the best MT response because the geological features have a dominant strike, therefore only the TM mode is considered in the discussion. This figure demonstrates clear uniformity between the observed and the modelled MT responses, and a distinctly different result for the seismic model. The error bars are set at 10 percent for the resistivity and 5 percent for phases. It should be noted that both the MT and seismic profiles have a similar shallow layer. Since, to a depth of 500 metres, both profiles do not have many features, we might expect the simplex method to produce similar curves in both cases because the algorithm is free to set the resistivities that minimise the RMS errors. From these examples, the MT profile is consistent with the soundings, while the seismic profile is not.

From Figure 8 we can make the following observations. The seismic model indicates zones of similar reflection characteristics. Our testable question focused on examining if zones of similar seismic reflectivity represent geological zones of similar electrical properties. On the basis of the plots, the connection between reflectivity and electrical resistivity is not supported, because the resistivity model based on the seismic profile does not match the inverted MT well. However, there is a resistivity model that can reproduce the data - the one provided by the MT block model. This implies one of two things: either the seismic interpretation is not geologically correct, or the link between the elasticity and the resistivity of the different geological zones is weak (which includes the possibly that there is similar structure in some regions but not others). However, this is conditional on the simplex method successfully minimizing χ^2. The

(a) Site 3 MT model

(b) Site 3 Seismic model

(c) Site 7 MT model

(d) Site 7 Seismic model

(e) Site 11 MT model

(f) Site 11 Seismic model
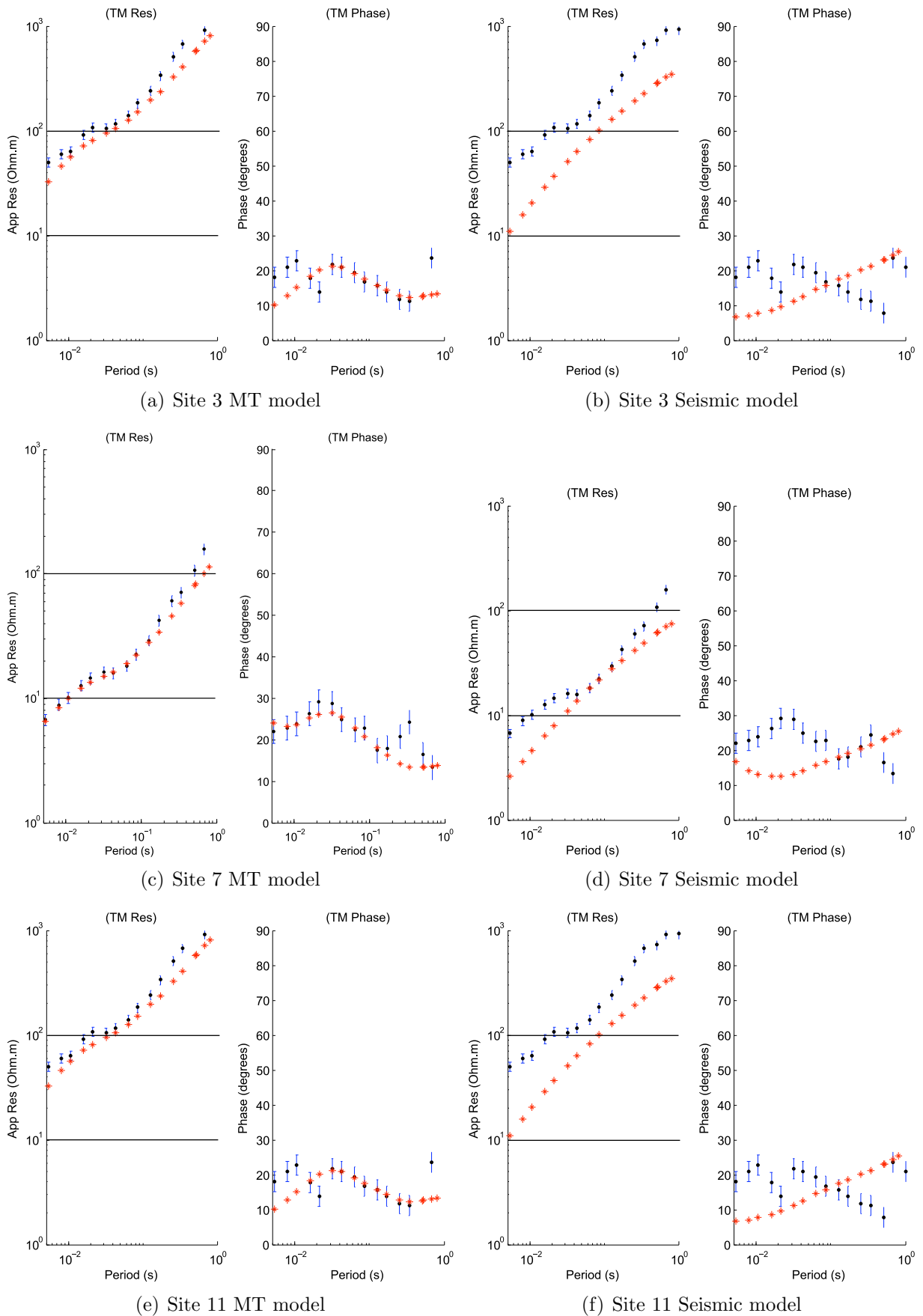
Figure 8: Soundings versus models (Blue=Soundings, Red=Model). The error bars are 10% for the resistivity diagrams and 5% for the phase diagrams. Continued next page...

(a) Site 13 MT model

(b) Site 13 Seismic model
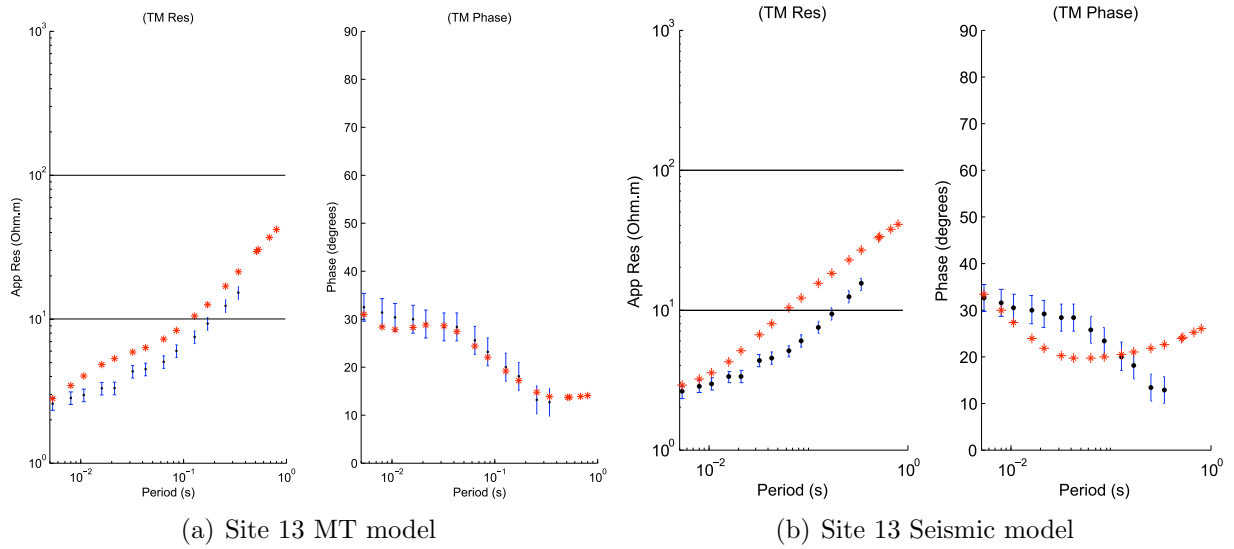
Figure 8: ...continued from previous page. The match between the Soundings and the MT model is good. The seismic model provides a poor match, especially the phase diagrams.

algorithm was run many hundreds of times to get the optimal results, but it is possible that a better solution exists. We face the issue not uncommon to joint inversion methods: the problems are ill-posed (non-linear, non-unique solutions or even no solutions at all) and there is the risk that the solution might iterate towards the wrong local minima.

Residuals

While Figure 8 provides a useful insight into the forward modelling at each instrument location, a better global picture is attained by examining residuals data. Figure 9 shows plots of the residuals (with a coloured scale) versus period along the length of the seismic line, for both resistivity and phase. The uniform colour scale of the MT residuals indicates a good fit. However, the MT model mismatch at site 4 stands out. MT does not tend to vary rapidly over such small distances, and clearly the match on either side is good. Since we are dealing with a relatively simple block model, this might indicate

(a) MT resistivity

PERIOD (s)	2	3	4	5	6	7	8	9	11	13	14
5.33E-03	-3.84	8.52	29.40	-1.30	6.77	0.53	-10.38	3.08	-3.09	-1.69	0.48
8.00E-03	-6.76	5.61	27.40	-3.06	5.77	1.16	-10.05	4.26	-3.81	-3.95	-1.73
1.07E-02	-8.53	2.38	24.65	-5.11	3.56	0.37	-10.76	3.87	-5.87	-6.14	-4.05
1.60E-02		4.95	24.67	-5.68	1.84	1.03	-10.08		-5.25	-7.56	-6.30
2.13E-02		5.72		-5.76		1.56			-6.24	-9.46	-8.27
3.20E-02	-10.34	2.09	23.80	-6.63	0.34	1.31		5.59	-3.56	-6.18	-2.61
4.27E-02	-10.28	1.92	22.21	-8.17	-1.36	-0.56	-11.07	3.87	-4.07	-6.86	-2.06
6.40E-02	-10.37	1.76	21.45	-9.10	-2.17	-0.93		4.11	-3.81	-7.29	-2.43
8.53E-02	-8.32	4.04	22.04	-8.42	-3.11	0.28	-9.74	4.98	-2.39	-6.55	-2.62
1.28E-01	-7.85	4.34	22.53	-7.88	-2.18	0.80	-8.90	6.04	-1.67	-6.70	-2.50
1.71E-01	-5.48	7.04	25.16	-5.30	-1.59	4.34	-5.14	9.05	0.23	-6.06	-2.80
2.56E-01	-4.62	9.05		-4.64	-1.82	5.55	-4.04	11.07	1.18	-6.28	-5.23
3.41E-01	-6.41	9.87	24.44	-6.03	-5.22	4.23	-5.50	10.53	1.26	-6.70	-8.32
5.12E-01	-8.91		24.62	-4.31			5.84	-4.56	9.95		
5.33E-01				-3.95							-5.34
6.83E-01		4.78		-1.37		9.06	-1.56	13.17			

(b) Seismic resistivity

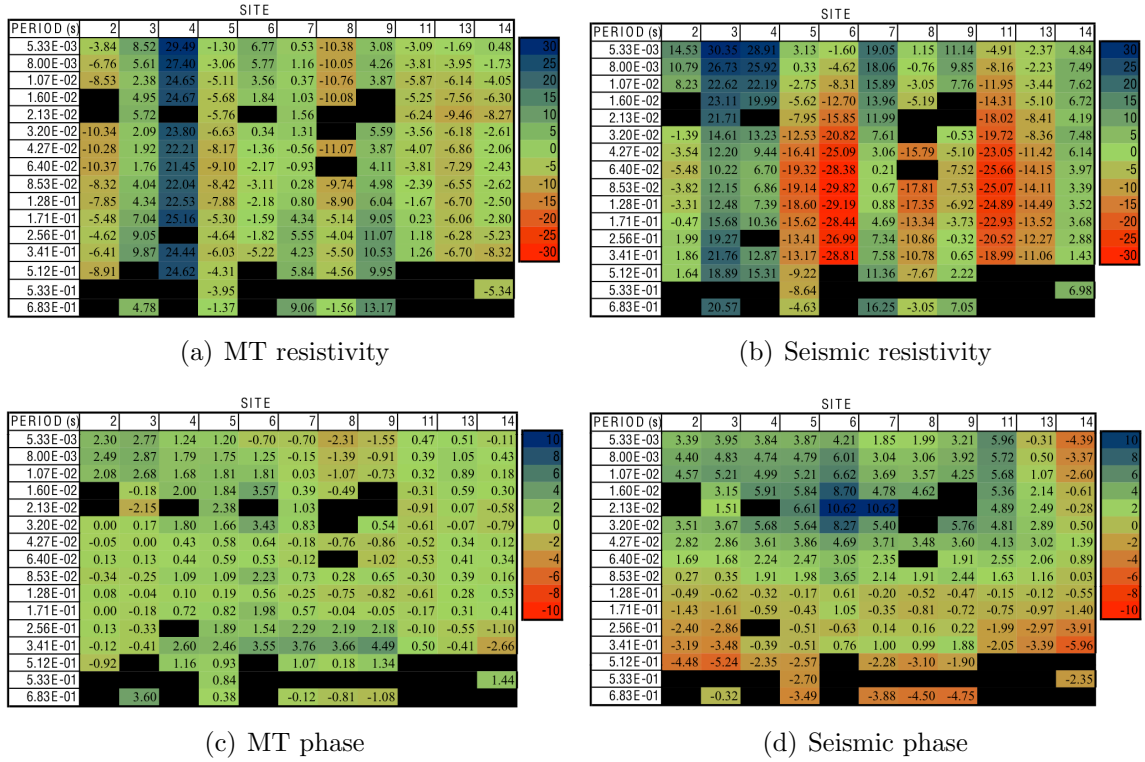| PERIOD (s)	2	3	4	5	6	7	8	9	11	13	14
5.33E-03	14.53	30.35	28.91	3.13	-1.60	19.05	1.15	11.14	-4.91	-2.37	4.84
8.00E-03	10.79	26.73	25.92	0.33	-4.62	18.06	-0.76	9.85	-8.16	-2.23	7.49
1.07E-02	8.23	22.62	22.19	-2.75	-8.31	15.89	-3.05	7.76	-11.95	-3.44	7.62
1.60E-02		23.11	19.99	-5.62	-12.70	13.96	-5.19		-14.31	-5.10	6.72
2.13E-02		21.71		-7.95	-15.85	11.99			-18.02	-8.41	4.19
3.20E-02	-1.39	14.61	13.23	-12.53	-20.82	7.61		-0.53	-19.72	-8.36	7.48
4.27E-02	-3.54	12.20	9.44	-16.41	-25.09	3.06	-15.79	-5.10	-23.05	-11.42	6.14
6.40E-02	-5.48	10.22	6.70	-19.32	-28.38	0.21		-7.52	-25.66	-14.15	3.97
8.53E-02	-3.82	12.15	6.86	-19.14	-29.82	0.67	-17.81	-7.53	-25.07	-14.11	3.39
1.28E-01	-3.31	12.48	7.39	-18.60	-29.19	0.88	-17.35	-6.92	-24.89	-14.49	3.52
1.71E-01	-0.47	15.68	10.36	-15.62	-28.44	4.69	-13.34	-3.73	-22.93	-13.52	3.68
2.56E-01	1.99	19.27		-13.41	-26.99	7.34	-10.86	-0.32	-20.52	-12.27	2.88
3.41E-01	1.86	21.76	12.87	-13.17	-28.81	7.58	-10.78	0.65	-18.99	-11.06	1.43
5.12E-01	1.64	18.89	15.31	-9.22		11.36	-7.67	2.22			
5.33E-01				-8.64							6.98
6.83E-01		20.57		-4.63		16.25	-3.05	7.05			

(c) MT phase

PERIOD (s)	2	3	4	5	6	7	8	9	11	13	14
5.33E-03	2.30	2.77	1.24	1.20	-0.70	-0.70	-2.31	-1.55	0.47	0.51	-0.11
8.00E-03	2.49	2.87	1.79	1.75	1.25	-0.15	-1.39	-0.91	0.39	1.05	0.43
1.07E-02	2.08	2.68	1.68	1.81	1.81	0.03	-1.07	-0.73	0.32	0.89	0.18
1.60E-02		-0.18	2.00	1.84	3.57	0.39	-0.49		-0.31	0.59	0.30
2.13E-02		-2.15		2.38		1.03			-0.91	0.07	-0.58
3.20E-02	0.00	0.17	1.80	1.66	3.43	0.83		0.54	-0.61	-0.07	-0.79
4.27E-02	-0.05	0.00	0.43	0.58	0.64	-0.18	-0.76	-0.86	-0.52	0.34	0.12
6.40E-02	0.13	0.13	0.44	0.59	0.53	-0.12		-1.02	-0.53	0.41	0.34
8.53E-02	-0.34	-0.25	1.09	1.09	2.23	0.73	0.28	0.65	-0.30	0.39	0.16
1.28E-01	0.08	-0.04	0.10	0.19	0.56	-0.25	-0.75	-0.82	-0.61	0.28	0.53
1.71E-01	0.00	-0.18	0.72	0.82	1.98	0.57	-0.04	-0.05	-0.17	0.31	0.41
2.56E-01	0.13	-0.33		1.89	1.54	2.29	2.19	2.18	-0.10	-0.55	-1.10
3.41E-01	-0.12	-0.41	2.60	2.46	3.55	3.76	3.66	4.49	0.50	-0.41	-2.66
5.12E-01	-0.92		1.16	0.93		1.07	0.18	1.34			
5.33E-01				0.84							1.44
6.83E-01		3.60		0.38		-0.12	-0.81	-1.08			

(d) Seismic phase

PERIOD (s)	2	3	4	5	6	7	8	9	11	13	14
5.33E-03	3.39	3.95	3.84	3.87	4.21	1.85	1.99	3.21	5.96	-0.31	-4.39
8.00E-03	4.40	4.83	4.74	4.79	6.01	3.04	3.06	3.92	5.72	0.50	-3.37
1.07E-02	4.57	5.21	4.99	5.21	6.62	3.69	3.57	4.25	5.68	1.07	-2.60
1.60E-02		3.15	5.91	5.84	8.70	4.78	4.62		5.36	2.14	-0.61
2.13E-02		1.51		6.61	10.62	10.62			4.89	2.49	-0.28
3.20E-02	3.51	3.67	5.68	5.64	8.27	5.40		5.76	4.81	2.89	0.50
4.27E-02	2.82	2.86	3.61	3.86	4.69	3.71	3.48	3.60	4.13	3.02	1.39
6.40E-02	1.69	1.68	2.24	2.47	3.05	2.35		1.91	2.55	2.06	0.89
8.53E-02	0.27	0.35	1.91	1.98	3.65	2.14	1.91	2.44	1.63	1.16	0.03
1.28E-01	-0.49	-0.62	-0.32	-0.17	0.61	-0.20	-0.52	-0.47	-0.15	-0.12	-0.55
1.71E-01	-1.43	-1.61	-0.59	-0.43	1.05	-0.35	-0.81	-0.72	-0.75	-0.97	-1.40
2.56E-01	-2.40	-2.86		-0.51	-0.63	0.14	0.16	0.22	-1.99	-2.97	-3.91
3.41E-01	-3.19	-3.48	-0.39	-0.51	0.76	1.00	0.99	1.88	-2.05	-3.39	-5.96
5.12E-01	-4.48	-5.24	-2.35	-2.57		-2.28	-3.10	-1.90			
5.33E-01				-2.70							-2.35
6.83E-01		-0.32		-3.49		-3.88	-4.50	-4.75			

Figure 9: Comparison of MT and seismic model resistivity and phase residuals.

a problem with the instrument at site 4. This discrepancy is apparent in neither the MT response from WinGLink, nor the inverted 2D image. The use of forward modelling has highlighted an issue that was otherwise not apparent, and this application warrants further investigation.

We might reasonably have expected the MT model to have given an even better match. There are two stand out reasons why this did not occur. The first, as was noted earlier, is that Hillside is an industrial site, and background noise is evident in the soundings data. It can be seen that, while the MT block model curves are better than the seismic model curves, the match is by no means perfect. Secondly, although we have a distinct, multi-coloured MT profile created though inversion (see Figure 6), this does not ensure we can readily produce a corresponding, physically realistic MT block model. The physical

	1	2	3	4	5	6	7	8	9	10
10	14.47	10.84	9.78	9.51	9.53	9.66	9.81	9.98	10.13	10.28
9	13.98	10.35	9.29	9.04	9.07	9.20	9.36	9.53	9.68	9.83
8	13.46	9.81	8.76	8.52	8.55	8.69	8.84	9.01	9.17	9.31
7	12.90	9.22	8.17	7.92	7.96	8.09	8.25	8.41	8.56	8.70
6	12.31	8.59	7.51	7.25	7.27	7.39	7.56	7.70	7.85	7.98
5	11.71	7.93	6.79	6.49	6.48	6.58	6.72	6.86	6.99	7.11
4	11.16	7.33	6.10	5.70	5.63	5.68	5.77	5.87	5.98	6.09
3	10.90	7.10	5.74	5.19	4.98	4.91	4.92	4.95	5.00	5.06
2	11.48	8.14	6.80	6.15	5.78	5.56	5.43	5.34	5.28	5.24
1	15.81	13.33	12.35	11.81	11.47	11.24	11.07	10.94	10.84	10.75

Legend: 15, 14, 13, 12, 11, 10, 9, 8, 7, 6, 5, 4

Figure 10: Sensitivity analysis for zone 1 versus zone 2 (the top two layers). The vertical axis shows the initial zone one values and the horizontal axis is for zone two. The numerical values, and colour contours, are the zone one RMS errors after a single iteration.
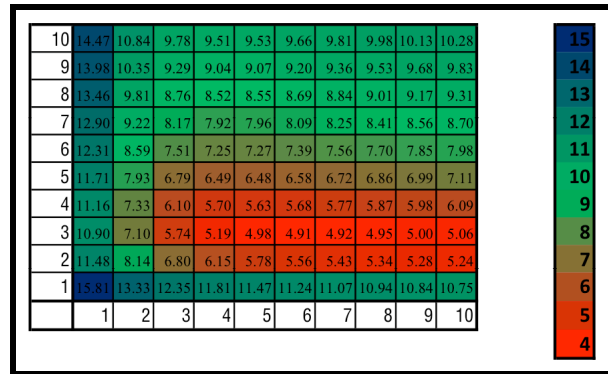
interactions that produce an MT response might not reduce well to a simple block model.

The problems in achieving a stronger match between the soundings data and the MT block model output may also indicate a limitation of the Nelder-Mead method. A different choice of initial resistivities may take us to different local minimum, or even a local minimum with resistivity and phase values that are physically impossible. We do not know, a priori, which initial values to choose. A better choice of resistivities or even a different search method may give a better global minimum. We must run the algorithm many times and pick the best solution. A major benefit of using the Nelder-Mead method is that it does not require derivatives and it is relatively easy to implement. Alternatively, a wide range of other search methods exist, including simulated annealing or genetic algorithms, that might lead to better results. Simulated annealing, for example, can be highly effective at avoiding these local minima in preference for the global minimum through a probabilistic approach to the problem .

Sensitivity Analysis

We would like to know something about the sensitivity of the solutions to perturbations. This gives an indication of the stability of a solution and can also show if a better solution exists. Figure 10 was created by running the simplex algorithm for a single iteration using the optimal solution for the initial zone values, taken from the MT block model.

In this example, the RMS of zone 1 is calculated against changes in zone 2. The vertical axis shows the initial zone 1 values and the horizontal axis is for zone two. The numerical values, and colour contours, are the zone one RMS errors after a single iteration. The initial zone 1 and zone 2 values are systematically changed from 1-10, keeping all other initial values from the optimal solution. The optimal resistivity values for zone 1 and zone 2 used throughout the previous sections were 2.8 and 7.6 respectively. The nearest block gives an RMS of 4.92, and is close to the local minimum of 4.91 found previously. Changing either of the initial resistivity values for zone 1 or 2 would results in the RMS value changing significantly for the worse.

Synthesis of MT and Seismic Data

Figure 11 shows MT and seismic inversion results at site 3. It has been selected because there appears to be a distinct regional boundary between two resistivity zones. Such a change in resistivity characteristics results in an accumulation of charge on the boundary that is well resolved by MT inversion. The existence of the MT boundary prompted further investigation of the seismic results, and upon closer inspection it can be seen that this boundary is evident within the seismic section also.

It is possible to use the MT to re-inform the seismic interpretation. On the basis of the MT at site 3, the seismic interpretation can be amended. Going in the other direction, since the boundary is clearly observable in the seismic section too, it may be valuable to set this as a fixed conducting boundary in running WingLink 2D inversion. While this is not an automated process, it is joint inversion. The MT data has changed the seismic interpretation, and the seismic data has changed the MT interpretation, leading to a better result in comparison to using each type of information independently.

Figure 11: This figure indicates the same features below site 3, observable in both the MT and the seismic response. The dotted vertical line was added to draw attention to the distinct vertical boundary between zones of similar elastic and electrical behaviour. The curved dotted lines mirror curved layering in both the MT and seismic measurements.
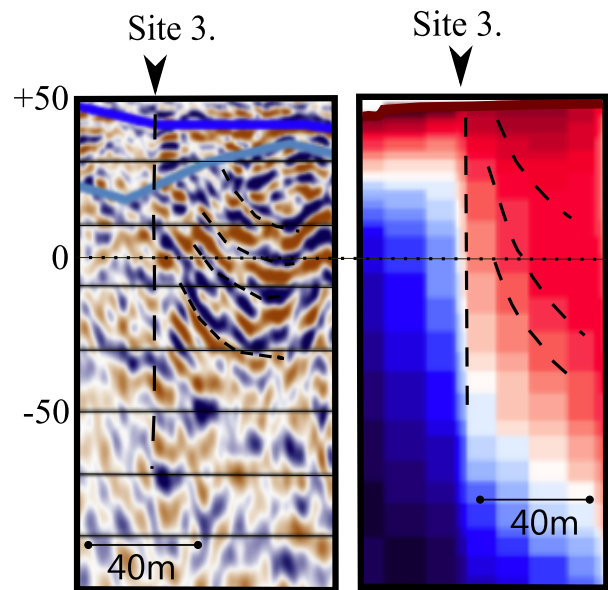
Comparison with other Geophysical Data

It is possible to use magnetic or gravity data to examine if zones of similar magnetic or density profiles represent geological zones of similar electrical properties. Since these data were unavailable, such a comparison must be left to further study. We would expect a closer connection between MT and magnetism or MT and density than MT and seismic data, since the underlying physical processes, equations and inversion processes are less disparate. Compared with seismic data, interpretation is also less subjective.

CONCLUSIONS

In this study, a new geometric based joint inversion method was developed. It was then used to examine the hypothesis that zones of similar reflectivity represent geological zones of similar electrical properties. Some of the typical issues of joint inversion were also discussed.

The approach we have taken is, in a limited sense, joint inversion (of a kind that Haber & Holtzman Gazit (2012) more precisely refer to as *model fusion*). However, conducting joint inversion was not our main focus. The emphasis in this study was on establishing whether or not zones of similar reflectivity represent geological zones of similar electrical properties. In a general sense, the answer is no. While there are at least two identifiable zone where such a connection appeared to exist, these are only local results indicating similar structure in some regions and not others.

Based upon all the observations, the joint inversion of MT and seismic data appears unlikely to be of great use in the geological setting of Hillside. While the results generally do not support a strong connection between MT and seismic results, this is based upon a single seismic interpretation. An alternative seismic interpretation, based upon different seismic characteristics, may yield a better result, and this is worth revisiting.

Within the confines of our approach, finding that there is not a strong geometric connection between MT and the given seismic interpretation is still a useful result. Joint inversion is widely assumed to improve the geological interpretation, but often improvements will be non-existent, or marginal at best. Since little literature exist on the limitations of joint inversion, this points the way to further research.

ACKNOWLEDGEMENTS

and assistance of *Rex Minerals* was an essential component of this study, and their contribution is greatly appreciated.

REFERENCES

Bosch, M. (1999). Lithological tomography: From plural geophysical data to lithology estimation, *Journal of Geophysical Research* **104**: 749–766.

Chave, A. & Thomas, D. (2003). A bounded influence regression estimator based on the statistics of the hat matrix, *J. Roy. Stat. Soc., Series C (Appl. Stat.)* **52**: 307–322.

Constable, S., Parker, R. L. & Constable, C. (1987). Occam's Inversion: A practical algorithm for generating smooth models from electromagnetic sounding data, *Geophysics* **52**(3): 289–300.

Fregoso, E. & Gallardo, L. (2009). Cross-gradients joint 3D inversion with applications to gravity and magnetic data, *Geophysics* **74**(4): L31–L42.

Gallardo, L. (2007). Multiple cross-gradient joint inversion for geospectral imaging, *Geophysical Research Letters* **34**(L19301): 1–5.

Gallardo, L. & Meju, M. (1997a). Characterization of heterogeneous near-surface materials by joint 2D inversion of dc resistivity and seismic data, *Geophysical Research Letters* **30**(13): 1658.

Gallardo, L. & Meju, M. (1997b). Joint 2D cross-gradient imaging of magnetotelluric and seismic travel-time data for structure and lithological classification, *Geophys. J. Int.* **169**(13): 1261–1272.

Gallardo, L. & Meju, M. (2004). Joint two-dimensional DC resistivity seismic travel time inversion with cross-gradient constraints, *Journal of Geophysical Research* **109**: 63–77.

Gallardo, L. & Meju, M. (2011). Structure-coupled multiphysics imaging in geophysical sciences, *Reviews of Geophysics* .

Gallardo, L., Meju, M. & Perez-Florez, M. A. (1997). A quadratic programming approach for joint image reconstruction: mathematical and geophysical examples, *Inverse Problems* **21**: 435–452.

Haber, E. & Holtzman Gazit, M. (2012). Model fusion and joint inversion, *Surveys in Geophysics* . Paper under review.

Haber, E. & Oldenburg, D. (1997). Joint Inversion: a structural approach, *Inverse Problems* **13**: 63–77.

Hoversten, M., Cassassuce, F., Gasperikova, E., Newman, G. A., Chen, J., Rubin, Y., Hou, Z. & Vasco, D. (2006). Direct reservoir parameter estimation using joint inversion of marine seismic AVA and CSEM data, *Geophysics* **71**(3): C1–C13.

Hu, W., Abubakar, A. & Habashy, T. M. (2009). Joint electromagnetic and seismic inversion using structural constraints, *Geophysics* **74**(6): R99–R109.

Linde, N., Biney, A., Tryggvason, A., Pedersen, L. B. & A., R. (2006). Improved hydrophysical characterization using joint inversion of cross-hole electrical resistance and ground-penetrating radar travel-time data, *Water Resour. Res.* **42**.

Linde, N., Tryggvason, A., Petersen, L. B. & Hubbard, S. (2008). Joint inversion of crosshole radar and seismic travel times acquired at the South Oyster bacterial transport site, *Geophysics* **73**(4): G29–G37.

Maier, R. (2011). *A Petrophysical Joint Inversion of Magnetotelluric and Gravity Data for Enhanced Subsurface Imaging of Sedimentary Environments*, PhD thesis, Earth and Environmental Science, University of Adelaide.

Michael Hoversten, G., Chen, J., Rubin, Y., Hou, Z. & Vasco, D. (2007). A Bayesian model for gas saturation estimation using marine seismic AVA and CSEM data seismic AVA and CSEM data, *Geophysics* **72**(2): WA85–WA95.

Nelder, J. & Mead, R. (1964). A simplex method of function minimization, *Computer Journal)* **7**: 308–313.

Parker, R. & Whaler, K. (1981). Numerical methods for establishing solutions to the inverse problem of electromagnetic induction., *J. Geophys. Res.* .

Pilkington, M. (2006). Joint inversion of gravity and magnetic data for two-layer models, *Geophysics* **71**(3): L35–L42.

Press, W., Teukolsky, S., Vetterling, W. & Flannery, B. (2007). *Numerical Recipes: The Art of Scientific Computing*, 3 edn, Cambridge University Press.

Raiche, A., Jupp, D., H., R. & Vozoff, K. (1985). The joint use of coincident loop transient electromagnetic and Schlumberger sounding to resolve layered structures, *Geophysics* **50**(10): 1618–1627.

Rodi, W. & Mackie, R. (2001). Non-linear conjugate gradient algorithms for 2-D magnetotelluric inversion, *Geophysics* **66**(1): 174–187.

Telford, W., Geldart, L. & Sheriff, R. (1990). *Applied Geophysics*, Cambridge University Press.

Tryggvason, A. & Linde, N. (2006). Local Earthquake (LE) tomography with joint inversion for P- and S-wave velocities using structural constraints, *Geophys. Res. Lett.* **33**.

Vozoff, K. & Jupp, D. (1975a). Joint Inversion of Geophysical Data, *Geophys. J.R. astr. Soc.* **42**: 977–991.

Vozoff, K. & Jupp, D. (1975b). Stable Iterative Methods for the Inversion of Geophysical Data, *Geophys. J.R. astr. Soc* .

Wannamaker, P., Stodt, J. & Rijo, L. (1987). A stable finite element solution for two-dimentional magnetotelluric modelin, *Geophys. J.R. astr. Soc.* **88**: 277–296.

White, A. & Heinson, G. (1994). Two-dimensional electrical conductivity structure across the southern coastline of Australia, *Journal of Geomagnetism and Geoelectricity* **46**: 1067–1081.

Appendices

APPENDIX A: This Appendix gives the location of the seismic line within the MT survey, and the coordinates of MT instruments along the seismic line.
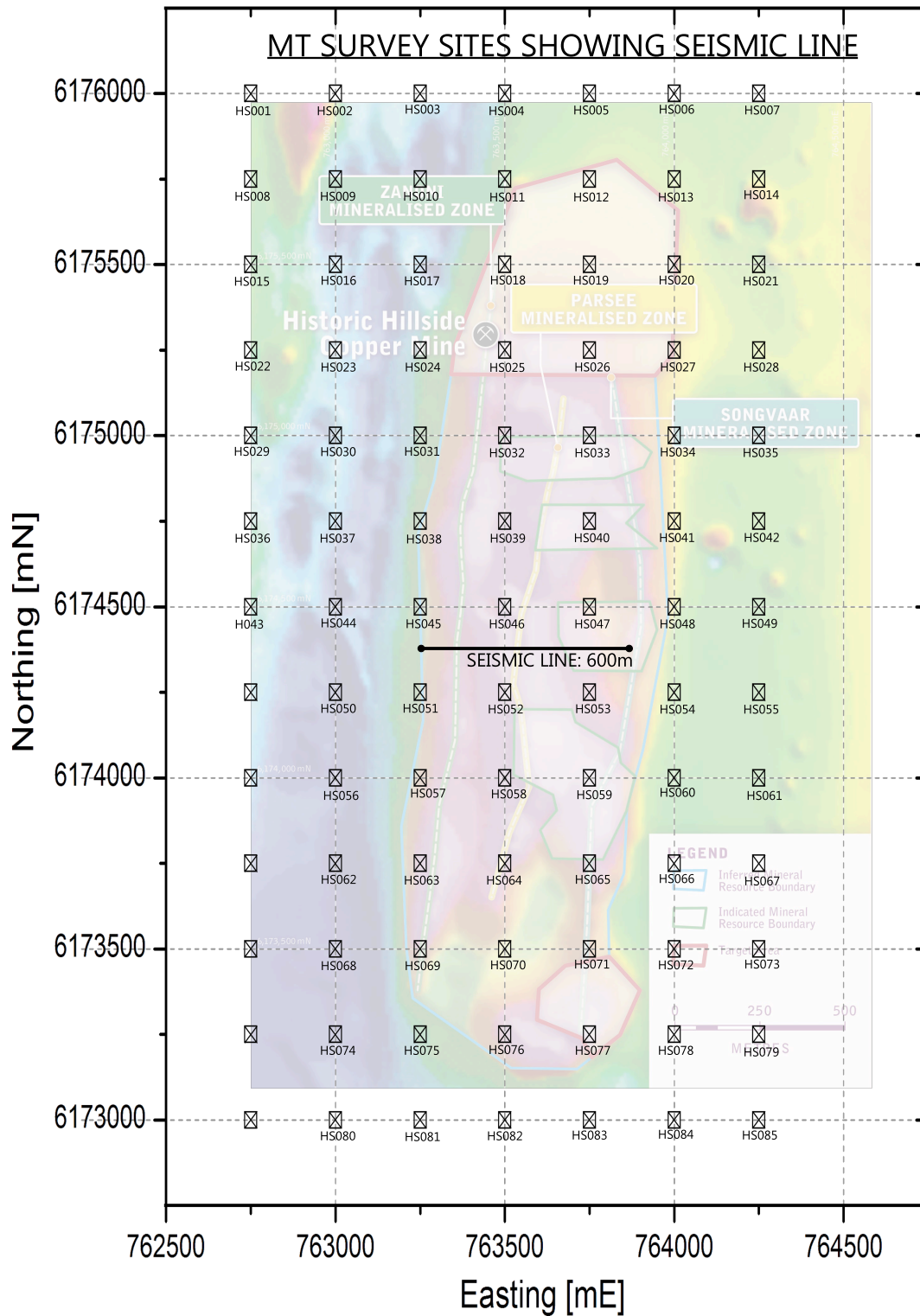
Hillside Seismic Line (HSSL)
Decimal Coordinates

Station	Long (°)	Lat (°)	Elevation (m)	Easting	Northing
HSSL01	137.86760	-34.53845	47	763174	6174403
HSSL02	137.86870	-34.53845	53	763274	6174401
HSSL03	137.86927	-34.53838	50	763327	6174406
HSSL04	137.86978	-34.53840	51	763373	6174403
HSSL05	137.87035	-34.53837	53	763427	6174404
HSSL06	137.87092	-34.53838	56	763477	6174402
HSSL07	137.87147	-34.53838	50	763529	6174401
HSSL08	137.87200	-34.53838	50	763578	6174400
HSSL09	137.87253	-34.53833	49	763627	6174402
HSSL10	137.87313	-34.53832	50	763677	6174404
HSSL11	137.87363	-34.53828	48	763727	6174406
HSSL12	137.87418	-34.53823	48	763778	6174411
HSSL13	137.87470	-34.53832	48	763826	6174401
HSSL14	137.87523	-34.53830	45	763875	6174400
HSSL15	137.87633	-34.53828	48	763975	6174399